



Perspective article

Patterned hydrophobic and hydrophilic surfaces of ultra-smooth nanocrystalline diamond layers



M. Mertens ^{a,*}, M. Mohr ^a, K. Brühne ^a, H.J. Fecht ^a, M. Łojkowski ^b, W. Święszkowski ^b, W. Łojkowski ^c

^a Institute of Micro and Nanomaterials, Ulm University, 89081 Ulm, Germany

^b Faculty of Materials Science and Engineering, Warsaw University of Technology, Warsaw, Poland

^c Institute of High Pressure Physics, Polish Academy of Sciences, Warsaw, Poland

ARTICLE INFO

Article history:

Received 6 June 2016

Received in revised form 1 August 2016

Accepted 24 August 2016

Available online 27 August 2016

Keywords:

Nanocrystalline diamond

HFCVD

Micropatterning

Microbiological investigations

ABSTRACT

In this work, we show that ultra nanocrystalline diamond (UNCD) surfaces have been modified to add them hydrophobic and hydrophilic properties. The nanocrystalline diamond films were deposited using the hot filament chemical vapor deposition (HFCVD) technique. This allows growing diamond on different substrates which can be even 3D or structured. Silicon and, for optical applications, transparent quartz glass are the preferred substrates for UNCD layers growth. Fluorine termination leads to strong hydrophobic properties as indicated by a high contact angle for water of more than 100°. Hydrogen termination shows lesser hydrophobic behavior. Hydrophilic characteristics has been realised with oxygen termination. X-ray photoelectron spectroscopy (XPS) and energy dispersive X-ray spectroscopy (EDX) measurements confirm the oxygen and fluorine- termination on the nanocrystalline diamond surface. Further, by micropatterning using photolithography, multi-terminated layers have been created with both hydrophobic and hydrophilic areas. In addition, we have shown that retermination is achieved, and the properties of the surface have been changed from hydrophobic to hydrophilic and vice versa. Micro-roughness and stress in the grown film influences slightly the wetting angle as well. The opportunity to realize local differences in hydrophobicity on nanocrystalline diamond layers, in any size or geometry, offers interesting applications for example in microbiological investigations. Multi-terminated arrays show identical surface roughness and at the same time differences in hydrophobicity. These arrays have been visualized with scanning electron microscopy (SEM) and lateral force microscopy (LFM).

© 2016 The Authors. Published by Elsevier B.V. This is an open access article under the CC BY-NC-ND license (<http://creativecommons.org/licenses/by-nc-nd/4.0/>).

1. Introduction

Diamond and, in particular ultra nanocrystalline diamond (UNCD) is well known for its excellent mechanical, electrical and optical properties. This is already integrated in some applications and available in several hybrid products [1]. The UNCD layers presented in the present paper are created using a hot filament chemical vapor deposition (HFCVD) technique, which allows growing diamond films with a wide range of grain size, from polycrystalline diamond with grain size in the micrometer range to nanocrystalline diamond. Nanocrystalline diamond layers with grain size in the range of 10 nm are further called UNCD. The HFCVD technique allows upscaling of UNCD layers production with high efficiency. UNCD can be deposited on different suitable sub-

strates which even can exhibit three dimensional surface elements. The surface of the substrate can be scaled up to several hundred square centimeters in size, which makes this technique flexible and therefore preferred in comparison with other diamond coating techniques. Primarily silicon wafers are used as substrate, but also quartz glass or carbide forming metals can be used. With changing growth parameter, for example by adding additionally other gases like oxygen, nitrogen, ammoniac or argon, it is possible to influence the grain size as well as the ratio between sp^2 to sp^3 bonded carbon in the grown film [2]. The roughness of UNCD is in the nano-scale and can be influenced by the growth conditions [2]. The nano-roughness is dependent on the grain size, film thickness, grain orientation, texture or surface treatments. Another very interesting field of research is the chemical surface modification of diamond by plasma techniques. UNCD surface termination with hydrogen, fluorine or oxygen have been reported in [3–7], which only represents a few examples of the resent years. With fluorine or hydrogen termination surface shifts towards the

* Corresponding author.

E-mail address: michael.mertens@uni-ulm.de (M. Mertens).

hydrophobic regime, while oxygen termination makes the surface more hydrophilic. Careful control of UNCD surface termination can change the contact angle in wide range from 10° to 100° [8,9]. Diamond is chemically inert and is stable to almost any acids. Diamond is also known as a biocompatible material [10]. Biocompatibility is a broad area of research with different applications. Histocompatibility, hemocompatibility or even microbiological cell growth on diamond substrate are topics of interest [10–13]. Biocompatibility can be generally influenced by surface properties like hydrophobicity, roughness or stiffness [14,15]. UNCD is an extremely stiff with Young's modulus varying with grain size from around 400 GPa to around 750 GPa [16]. High stiffness and it consistency is a preferable surface for many cell subtypes, as it promotes stable cell, surface adhesion, and therefore cells spreading and proliferation [17]. Moreover UNCD offers the possibility to conduct research on substrates that have consistent roughness and stiffness along whole surface, and this parameters are not affected by softening or swelling by exposure to culture media, which is important for the reproducibility of results [18].

As we show in this work, by combining termination with photolithography it is possible to create hydrophilic-hydrophobic arrays referred here as multi-termination, which show identical surface roughness. Such arrays possess wide application in areas of: microfluidics, high-throughput screenings, drug testing or cell microarrays [19,20].

2. Experimental methods

UNCD films with a thickness of typically 1 μm were grown on a silicon substrate by hot filament chemical vapor deposition (HFCVD). To induce the initial heterogeneous nucleation event for the diamond growth, the silicon substrate is appropriately seeded [1]. After seeding the substrate in a water bath with nanodiamonds it is placed in front of the tungsten filaments in the growth chamber. For the growth of UNCD the most important parameters are gas composition of methane and hydrogen and the substrate temperature. In this case the methane/hydrogen gas flow was 3% and the substrate temperature was about 570 °C. The filament temperature of about 2000 °C leads to an activation of hydrogen to atomic hydrogen. One three inch silicon wafer was coated with about 1 μm UNCD and then divided into three similar pieces. Directly after the growth process the diamond surface is hydrogen terminated, because of the hydrogen atmosphere present during the growth.

We used two different ways to generate an oxygen termination. The first one was the chemically modification of the surface by piranha acid ((H₂O₂)_{0.33}:(H₂SO₄)_{0.66}). This treatment leads to an oxygen termination on the surface and is often also used as cleaning process. Independent from the chemical approach the second way to generate an oxygen termination is an oxygen plasma process. The plasma is burned in a barrel reactor under room temperature conditions, with a typically process pressure of 0.1 mbar, a flow of 10 sccm O₂ and a power of 100 W with a frequency for the plasma modification of 13,56 MHz. The third investigated termination was fluorine. This surface termination can be also generated with plasma process in a barrel reactor. In this case a CF₄-gas is used, with a process pressure of 0.3 mbar and a gas flow of 50 sccm.

We attempted as well the realization of two different terminations on one UNCD-surface. A step towards this goal was to change a termination from hydrophobic fluorine termination to hydrophilic oxygen termination which we refer as retermination. This offers for example locally preferred living conditions for biological cells, which is interesting for microbiological investigations. We performed the retermination in a plasma process at room temperature. One sample was first fluorine terminated and then reterminated in pure oxygen plasma for 10 min.

In order to produce samples with both hydrophobic and hydrophilic terminations (multiple-terminations) we started from a fluorine terminated sample. With a photo-lithography process, the surface is partially covered with developed photoresist. In this case a typical image reversal photoresist (AZ-5214) was used, with a thickness of about 1 μm. After the photo-lithography process the sample is exposed to pure oxygen plasma. The photoresist works as protection for the fluorine termination. On the positions without protection the fluorine terminations gets removed within 5–10 min and replaced by an oxygen termination. Finally the resist on top of the fluorine terminations gets removed by using solvents, acetone and the developer AZ726 was used. Both solvents were previously tested on a fluorine terminated sample with no influence on hydrophobicity. Due to the used photo-lithography technique, multiple terminated – micropatterned areas can be realized in any desired size or geometry down to the micrometer range.

To record and to quantify the hydrophobicity the water contact angle φ for water was measured. This measurement method is based on the Young's equation

$$\cos(\phi) = \frac{\sigma_S - \sigma_{LS}}{\sigma_L}, \quad (1)$$

which describes the relationship between specific surface energy of the solid σ_S, interfacial energy between solid and liquid σ_{LS} and surface energy of water σ_L. In the experiment water drops are placed on the diamond film. The water drops always have the same mass of water and the dropping height is also fixed. A camera takes pictures of these water drops, which is mounted on the same horizontal height than the sample surface. The water angle can be directly extracted from the picture and allows a quantitative comparison of hydrophobicity. To get statistics and to investigate secondary influences on hydrophobicity, this process is repeated on different positions on the sample.

The average grain size of the UNCD films was measured by means of X-ray diffraction using the Scherrer's formula was between 9 to 11 nm.

The surface termination was verified by means of X-ray photoelectron spectroscopy (XPS). An aluminum anode without monochromator was used. The measurement resolution was about 0.5 eV. The binding energy was calibrated using the signal of the Au 4f duplet from the sample holder. The spectrum was measured in the range of binding energies from 250 eV to 800 eV. Further, energy dispersive X-ray spectroscopy (EDX) measurements were done. The used acceleration voltage of 5 kV leads to a penetration depth of 300 nm.

Atomic Force Microscopy (AFM) Asylum Research MFP3D Bio was used to determine the surface roughness, and to perform Lateral Force Microscopy (LFM) to observe the differences in surface friction for different terminations. The friction between tip and surface is generated by surface roughness but also by the work of adhesion between tip and surface due to atomic interactions and therefore it can be used to image areas of different chemical properties [21]. The LFM signal corresponds to the torsion of the cantilever, caused by friction, when the cantilever slides on the sample surface in lateral direction [21]. Imaging was performed in contact mode in air. An Olympus RC800PSA cantilevers were used. Cantilevers were calibrated with GetReal™ algorithm implemented to AFM software provided by Asylum Research. The cantilevers spring constant ranged from 0,6 N/m to 0,7 N/m.

3. Results and verification

Fig. 1 shows the contact angle of the oxygen-, fluorine- and the hydrogen terminated diamond surface in one graph. The arithmetic average of about 20 positions on each sample, with a sample size of about 10 square centimeters is shown. Additionally the stan-

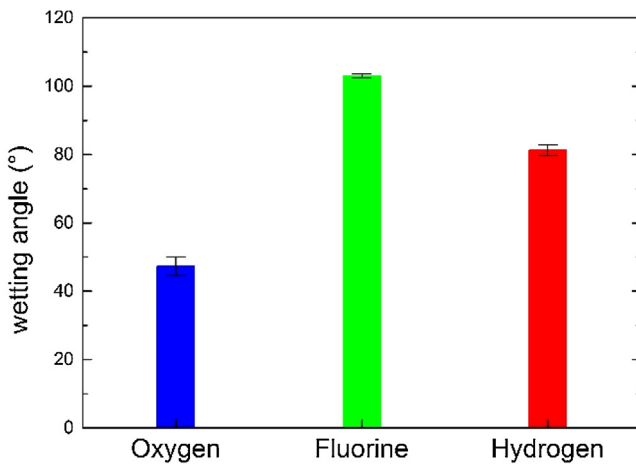


Fig. 1. The contact angle for water depending on oxygen, fluorine and hydrogen terminated ultra-nanocrystalline diamond films. The oxygen termination shows hydrophilic properties with an average contact angle of 47.2° . In contrast the hydrogen termination leads to a contact angle of 81.3° and the fluorine termination shows maximum hydrophobic properties with a contact angle of 103° .

dard deviation of all the measurement points is added. The oxygen terminated sample, which was chemically terminated shows the most hydrophilic properties, with a wetting angle in the range from 42.3° to 51.4° . The fluorine terminated sample illustrates the exact opposite, on a direct comparable diamond film like the first one. In this case the wetting is between 101.8° and 103.9° . These big contact angles show the water repelling characteristics, thus the hydrophobic properties of fluorine terminated UNCD surfaces. The third sample, the hydrogen terminated sample also shows slightly hydrophobic properties with wetting angles between 78.5° and 83.9° . The above results are in agreement with several publications e.g. [22,8]. Oxygen leads to hydrophilic properties and in contrast hydrogen and fluorine to hydrophobic properties.

As seen in the previous results (Fig. 1) a range of wetting angles was measured for each termination. The oxygen terminated sample showed a difference of about 10° between various positions, which shows the plotted error bar. In contrast the fluorine termination showed only a minor of variation. The hydrogen, the sample with no further treatments at all after growth shows also variations in the wetting behavior. We attributed these small variations of the wetting angle as function of the distance from the wafer center to variations of roughness. Also the film thickness changes as function of the distance which might lead to intrinsic stress in the grown film. The UNCD film roughness, as well as the film thickness is slightly varying as a function of distance from the sample center $R_{\text{RMS}} = 9.5 \text{ nm}$ to $R_{\text{RMS}} = 12.1 \text{ nm}$. In that range the thickness differs between about $1 \mu\text{m}$ and $1.3 \mu\text{m}$ as well. The slight differences in nano-roughness of the surface and growth rate results from small differences in growth conditions of the nanocrystalline diamond films, caused by primarily temperature gradients. No significant difference in roughness between O – termination and F – termination was observed. For all samples, with increasing roughness and thickness the hydrophobicity increases. The general effect of roughness to hydrophobicity is known [23]. The oxygen terminated sample showed the largest difference in roughness and thickness and therefore in hydrophobicity. The fluorine terminated sample showed the smallest absolute deviation, because of more homogeneous film properties on that sample area. The influence of these effects is insignificant compared to the difference in hydrophobicity, which can be achieved by different surface termination.

Fig. 2 shows the results of the XPS-measurement on the fluorine terminated sample. Clearly identifiable is the carbon 1s peak at 285 eV and the fluorine 1s at 688 eV [24]. On the right side of the

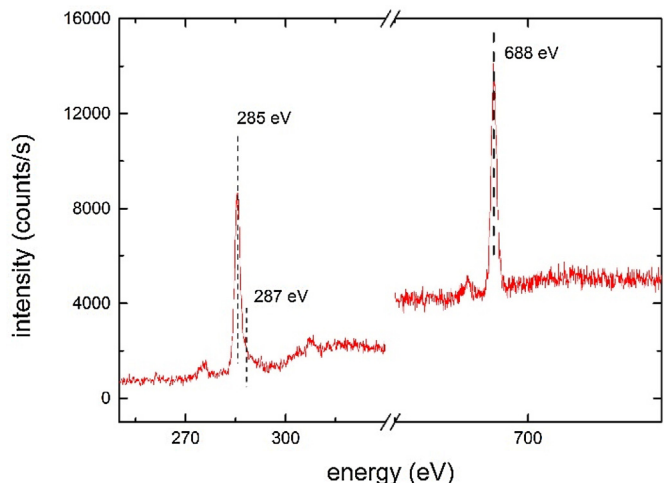


Fig. 2. XPS-measurement of the fluorine terminated sample, with marked peaks at 285 eV (carbon 1s), 287 eV (carbon fluorine bond) and 688 eV (fluorine 1s).

carbon 1s is a small shoulder. The corresponding peak at 287 eV gives the hint to existing carbon fluorine bonds [24].

EDX measurements also show the presence of fluorine on the sample, of about 0.4 at%. This indicates more fluorine on the surface, than just one single bonded fluorine monolayer on the surface.

After observing the absolute difference between hydrophilic and extreme hydrophobic properties by applying different terminations, we attempted the realization of two different terminations on one UNCD-surface.

The retermination procedure resulted in a change from hydrophobic behavior to hydrophilic reaction. Directly after the fluorine termination the sample showed wetting angles above 100° (Fig. 1). After the retermination the sample shows angles between 71.4° to 81.44° . Within 10 min oxygen plasma treatment it was however not possible to reach the same hydrophilic properties as for a pure (chemical modification) oxygen terminated sample. The time in the oxygen plasma is reduced to a minimum, to avoid etching the diamond [25]. Long exposures in the oxygen plasma would lead to more hydrophilic properties and to a significant smoothening of the surface. As consequence the roughness would be incomparable to the as-grown and to the fluorine terminated sample. Fig. 3 shows the XPS measurements on the reterminated fluorine terminated sample after 10 min oxygen plasma treatment. In the measured range the carbon 1s peak and the oxygen peak at 532 eV can be seen. The oxygen peak on the fluorine terminated sample appears due to atmospheric adsorbents on the sample surface [26]. The initially observed fluorine 1s peak, at 688 eV decreased drastically but is still detectable with a small shift towards 686 eV , what can be attributed to a small fraction of semi-ionic carbon-fluorine bonds that remain as residues of fluorine on the surface. This explains the remaining hydrophobic properties.

Fig. 4 shows SEM pictures of the hydrophilic and hydrophobic micropatterned areas. The picture with the higher magnification b) shows a shape contrast which confirms the quality of micropatterning. There is a contrast between the two different terminated areas due to differences in the surface electrical conductivity and electron affinity as a function of termination.

The Lateral Force Microscopy measurements shows in Fig. 5b) that friction in hydrophobic, fluorine terminated area is higher (Table 1 and Fig. 5b)) than in oxygen terminated area, while the roughness in both areas is same as shown on Fig. 5a). In the AFM Lateral Force Microscopy mode the cantilever slides on the sample surface in lateral direction, and every change in surface friction is transformed into lateral bending of the cantilever which is then

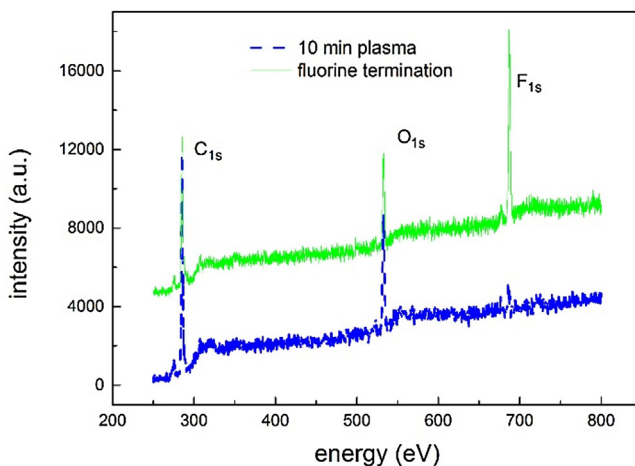


Fig. 3. Comparison of two XPS-measurements, before and after retermiantion: Fluorine terminated sample (green, upper curve) and the reterminated sample after 10 min oxygen plasma treatment (blue, dashed lower curve). The initial fluorine 1s peak at 688 eV became considerable smaller after the oxygen plasma and shifted towards a lower energy of 686 eV. (For interpretation of the references to color in this figure legend, the reader is referred to the web version of this article.)

Table 1

Micropatterned NCD roughness corresponding to Fig. 5b), measured by lateral force microscopy (LFM). The fluorine terminated area shows slightly higher friction in contrast to the surrounding oxygen area. The hydrogen terminated UNCD surface (as-grown) for compassion shows 12.1 nm surface roughness.

	Fluorine area	Oxygen area
Average deviation R_a	11.6 nm	11.4 nm
Standard deviation R_q	14.8 nm	14.5 nm

transmitted by reflection of the laser on the photodiode and represented as a voltage output [21]. The AFM topographic image Fig. 5 a) shows no difference between the fluorine and the oxygen terminations.

To visualize a multi-terminated surface, a thin water film is spray coated on the UNCD surface. In Fig. 6 one example of a multi-terminated UNCD surface is shown. Round structures are projected which are oxygen terminated. These round structures with a diameter of about 200 μm are surrounded by a fluorine termination. The water gathers primarily to the areas which are attractive to water, due to their higher hydrophilic properties. The water repelled areas additionally keep the water to the hydrophilic areas. This visualization technique also shows clearly the presence of different terminations, beside the SEM pictures. The used photo-lithography

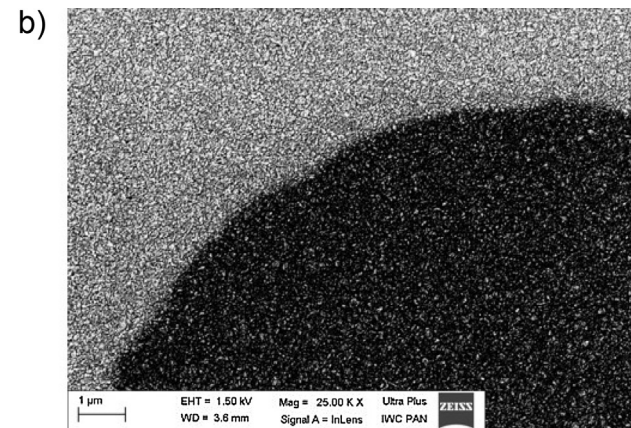
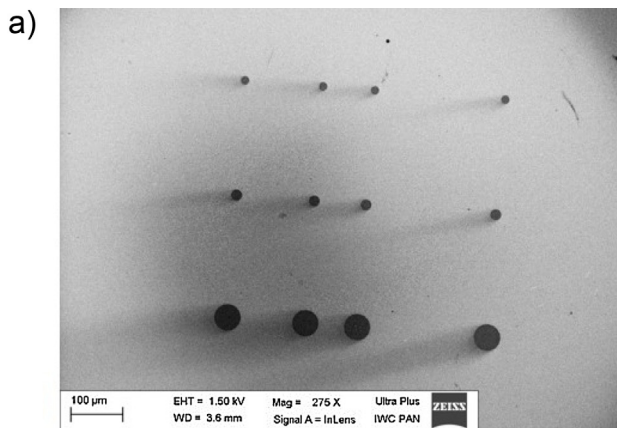


Fig. 4. a) SEM picture of micro patterned fluorine terminated areas with different diameters (15 μm , 20 μm and 50 μm) in oxygen surrounding, b) high magnification of one multi-terminated micropatterns. The contrast between oxygen and fluorine is visible, because of different surface electrical conductivity.

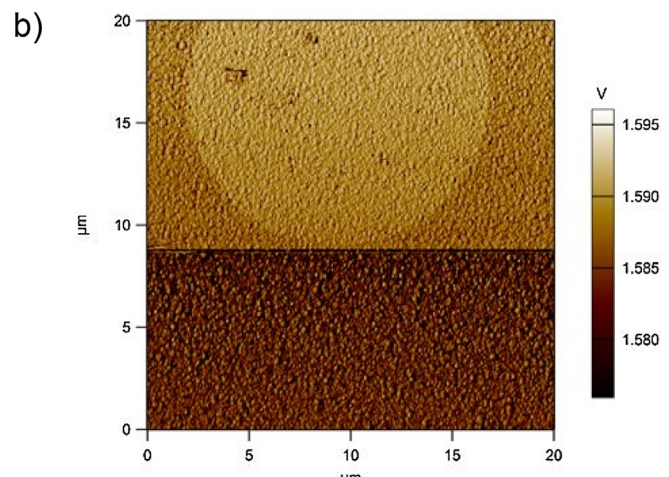
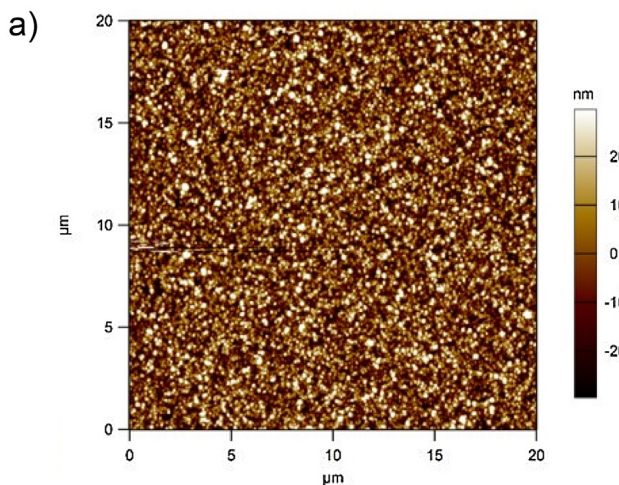


Fig. 5. a) Topographic image of micropatterned NCD measured by AFM, which shows homogenous surface roughness b) The same region imaged measured with LFM, with a visible contrast of the micropattern. Brighter area means higher friction in the area with the fluorine termination.

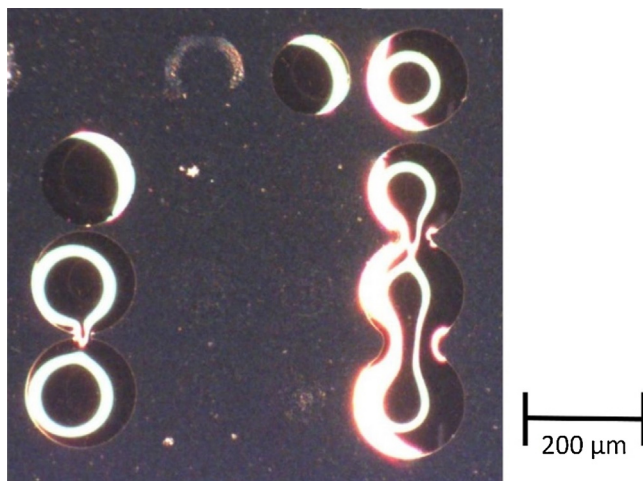


Fig. 6. Visualization of a multi terminated surface, by a thin water film. Round oxygen terminated spots with a diameter of $200\text{ }\mu\text{m}$ surrounded by a fluorine termination. The water gathers to the oxygen terminated areas.

technique allows the realization of multi terminated surfaces in any desired size or geometry.

4. Summary

In conclusion, hydrophilicity on ultra-smooth nanocrystalline diamond layers can be controlled by varying the surface termination: oxygen, hydrogen and fluorine. Hydrophilic properties can be achieved by oxygen termination, while hydrogen and fluorine are showing hydrophobic characteristics. Fluorine leads to strongly hydrophobic properties, with wetting angles over 100° . Minor surface roughness and stress variations in the grown film has small influences on hydrophilicity.

Photo-lithography technique allows the realization of a multi-terminated surface on nanocrystalline diamond layers. It is also possible to replace terminations and to change therefore the hydrophilicity. The presented technique offers the opportunity to realize two different terminations on one sample, in any desired geometry or size down to the micrometer range. This could lead to many applications, from MEMS coatings, arrays for microbiological studies, microfluidic biosensors, or even sun energy harvesting. Stiff, smooth, and biocompatible surfaces, that possess the same roughness regardless of the wetting angle will permit good receptiveness for microbiological studies.

Acknowledgments

The authors gratefully acknowledge the financial support by the German ministry of education and research (BMBF) through VDI/VDE-IT, within the project VIP-DiM (FKZ 16SV6503) and also the National Centre for Research and Developments (Grant No. STRATEGMED1/233224/10/NCBR/2014; Project START).

References

- [1] H.-J. Fecht, K. Brühne, P. Gluche, Carbon-based nanomaterials and hybrids—synthesis, in: Properties, and Commercial Applications, Pan Stanford Publishing, Singapore, 2014.
- [2] M. Wiora, K. Brühne, A. Flöter, P. Gluche, T. Willey, S.O. Kucheyev, A.W. Van Buuren, A.V. Hamza, J. Biener, H.-J. Fecht, Diamond Relat. Mater. 18 (2009) 927–930.
- [3] Y.-S. Park, H.-G. Son, D.-H. Kim, H.-G. Oh, D.-S. Lee, M.-H. Kim, K.-M. Lim, K.-S. Song, Appl. Surf. Sci. 361 (2016) 269–276.
- [4] L. Ostrovskaya, V. Perevertailo, V. Ralchenko, A. Saveliev, V. Zhuravlev, Diamond Relat. Mater. 16 (2007) 2109–2113.
- [5] I. Shpilevaya, J.S. Foord, Electroanalysis 26 (2014) 2088–2099.
- [6] C. Popov, H. Vasilchina, W. Kulisch, F. Danneil, M. Stüber, U.S.A. Welle, J.P. Reithmaier, Diamond Relat. Mater. 18 (2009) 895–898.
- [7] J. Miksovskya, A. Vossa, R. Kozarovad, T. Kocourek, P. Pisarik, G. Cecconee, W. Kulisch, M. Jelinek, M.D. Apostolovad, J.P. Reithmaiera, C. Popova, Appl. Surf. Sci. 297 (2014) 95–102.
- [8] L. Yang, Y. Li, B.W. Sheldon, T.J. Webster, J. Mater. Chem. 22 (2012) 205.
- [9] T. Lechleitner, F. Klauser, T. Seppi, J. Lechner, P. Jenning, P. Preco, B. Mayer, D. Steinmüller-Nethl, J. Preiner, P. Hinterdorfer, M. Hermann, E. Bertel, K. Pfaller, W. Pfaller, Biomaterials 29 (2008) 4275–4284.
- [10] C. Tsai, W.W. Gerberich, L. Kruckeberg, D.R. Kania, Biomaterials 16 (483–488) (2016) 2995.
- [11] F. Klauser, M. Herman, D. Steinmüller-Nethl, O. Eiter, A. Pasquarelli, E. Bertel, T. Seppi, P. Lukas, T. Lechleitner, Chem. Vap. Deposition 16 (2010) 42–49.
- [12] M. Kalbacova, L. Michalikova, V. Baresova, A. Kromka, B. Rezek, S. Kmoch, Phys. Status B 245 (2008) 2124–2127.
- [13] P. Bajaj, D. Akin, A. Gupta, D. Sherman, B. Shi, O. Auciello, R. Bashir, Biomed. Microdevices 9 (2007) 787–794.
- [14] H.-I. Chang, Y. Wang, Cell responses to surface and architecture of tissue engineering scaffolds, in: Regenerative Medicine and Tissue Engineering – Cells and Biomaterials, InTech, 2011.
- [15] A.J. Engler, S. Sen, H.L. Sweeney, D.E. Discher, Cell 126 (2006) 677–689.
- [16] M. Mohr, A. Caron, P. Herbeck-Engel, R. Bennewitz, P. Gluche, K. Brühne, H.-J. Fecht, J. Appl. Phys. 116 (2014).
- [17] H.-J. Chang, Y. Wang, Regenerative Medicine and Tissue Engineering—Cells and Biomaterials, InTech, 2011, 2016.
- [18] A.P. Sommer, M.K. Haddad, H.-J. Fecht, J. Bionic Eng. 9 (2016) 353–357.
- [19] J.S. Li, E. Ueda, A. Nallapaneni, L.X. Li, P. Levkin, Langmuir 28 (2012) 8286–8291.
- [20] A.N. Efremov, M. Grunze, P.A. Levkin, Adv. Mater. Intrefaces 1 (2014).
- [21] J.L. Wilbur, H.A. Biebuyck, J. MacDonald, G.M. Whitesides, Langmuir 11 (1995) 825–831.
- [22] W. Kulisch, C. Popov, D. Gilliland, G. Ceccone, L. Sirghi, A. Ruiz, F. Rossi, Diamond Relat. Mater. 18 (2009) 747–749.
- [23] R.N. Wenzel, J. Phys. Chem. 53 (1949) 1466–1467.
- [24] A. Tressaud, F. Moguet, S. Flandrois, M. Chambon, C. Guimon, G. Nanse, E. Papirer, V. Gupta, O.P. Bahl, J. Phys. Chem. Solids 57 (1996) 745–751.
- [25] H. Shiomi, J. Appl. Phys. 36 (1997) 7745–7748.
- [26] R. Akhvlediani, S. Michaelson, A. Hoffman, Surf. Sci. 604 (2010) 2129–2138.